Double-transmembrane domain reduces fusion rate by increasing lipid-protein mismatch

B. Bu[1], Z. Tian[2,3], D. Li[4,*], K. Zhang[5], B. Ji[4], J. Diao[2,*]

ABSTRACT: Membrane fusion mediated by Soluble N-ethylmaleimide-sensitive factor activating protein receptor (SNARE) proteins is an important cellular process. For neuronal SNAREs, the single transmembrane domain has been proposed to pass zippering energy to membranes for inducing fast fusion. In contrast, the SNARE protein, syntaxin 17, for membrane fusion involved in autophagosome maturation contains an unusual V-shape double-transmembrane domain that may influence its capability to pass energy. Here, we showed that this double-transmembrane domain significantly reduces fusion with an in vitro reconstitution system. Through theoretic modelling, we found that this V-shape

24 double-transmembrane domain increases lipid-protein mismatch, which reduces the energy transduction
25 for fusion. Moreover, our model also revealed the involvement of 2-3 SNAREs in a general fusion
26 process.
27
28 **RUNNING TITLE**: Transmembrane domain in fusion
29
30 **SIGNIFICANT STATEMENT**: Soluble N-ethylmaleimide-sensitive factor activating protein receptors
31 (SNAREs) serve as the molecular machine to mediate membrane fusion. The zipper formation of core
32 structure extending to membranes by two single transmembrena domains (TMDs) is the main driving
33 force of membrane fusion. The role of TMD in fusion is unclear. By adding an extra TMD, we found
34 that the hydrophobic mismatch effect between the thickness of the membrane and the length of TMDs
35 plays an important role in regulating fusion.
36

INTRODUCTION

As a ubiquitous cellular process, membrane fusion plays a decisive role in the neurotransmission, drug delivery, exo- and endocytosis (1-4). Soluble N-ethylmaleimide-sensitive factor activating protein receptors (SNAREs) serve as the molecular machine to mediate neurotransmission and other fusion process (5, 6). The core structure of neuronal SNAREs is compposed of synaptobrevin-2 (Syb 2, also called VAMP2: vesicle-associated membrane protein 2), syntaxin-1 (Syx 1), and SNAP-25. The C-terminal single transmembrane domain (TMD) of Syb 2 anchored on the synaptic vesicles and the C-terminal single TMD of Syx 1 located in the plasma membrane. They winded with SNAP-25 and formed a 4-helical SNARE core structure (7). The extenstion of the zipper formation of core structure to membranes by these two single TMDs is the main driving force of membrane fusion (8). Most SNARE proteins contain a single TMD except for syntaxin 17 (Syx 17) that contains unique V-shape double TMDs and serves in the fusion process between autophagosomes and lysosomes (9, 10) (**Fig. S1**). Determining the influence of Syx 17 double TMDs in membrane fusion is important for the mechanistic understanding of fusion regulation.

Membrane fusion can be regulated by the physicochemical property of the lipids and the structure of SNAREs (1, 11-16). For instance, Katsov et al. (11) investigated how lipid compositions influences fusion process, suggesting that lipids with spontaneous negative curvature (e.g. phosphatidylethanolamine (PE) and cholesterol (CHOL)) have a lower energy barrier to accomplish fusion process. Furthermore, Jackson took into account the deformation and motion of the membrane and SNAREs TMDs into a theoretical model and showed the impact of TMD properties (e.g. TMDs' stiffness and numbers) on the fusion energy profile and fusion rate (13). To the best of our knowledge,

most previous studies focused on the membrane or the SNAREs individually, the influence of lipid-SNAREs interaction on the fusion process is still unclear.

When SNAREs, particularly those containing transmembrane domains (TMDs) (e.g. Syb and Syx), insert into the membrane, a hydrophobic mismatch can occur between the lipid bilayer and TMDs due to different size of the lipid bilayer thickness and the length of TMDs. Such a hydrophobic mismatch could tilt the insertion angle of the axis of TMDs depending on the TMD's length and membrane composition (17-19). Consequently, this hydrophobic mismatch can affect the structure of TMDs, change the local distribution of SNAREs, and even influence the fusion rate (20, 21). Motivated by these results, we reason that lipid-SNAREs interaction can exert critical effects on membrane fusion. To date, however, rare model includes the lipid-SNAREs interaction in the mechanistic study of membrane fusion.

To study the role of TMD in membrane fusion, we used a new approach of adding TMD, which is different with previous assay of removing TMD (22). Through ensemble lipid-mixing and single-vesicle docking assays, we showed that a double TMDs from Syx 17 reduced the fusion rate about 4 times compared to a single TMD domain from the wildtype Syx 1 (Syx 1 WT). To explain this difference, we determined the effect of lipid-SNAREs mismatch on the membrane fusion process by introducing a theoretical model that treats lipid-protein interaction explicitly. This model shows that increased lipid-SNAREs mismatch should slow down the fusion process, which is supported by the experimental result that double TMDs reduce the membrane fusion rate. Our results provide both theoretical and experimental frameworks for the mechanistic study of the regulatory roles of lipid-SNAREs interaction involved in the membrane fusion process.

MATERIALS AND METHODS

Protein preparation

All proteins were from rat and expressed and purified as described by (23-25). Briefly, his-tagged Syx 1 WT, Syx 1/17 containing the cytoplasmic domain of Syx 1 and the double transmembrane domains of Sxy 17, Syb 2, and SNAP-25 were expressed in *E. coli* and purified using a combination of Ni-NTA affinity (Qiagen, Hilden, Germany) and size exclusion chromatography on a Superdex 200 column (GE Healthcare, Uppsala, Sweden). His-tags were removed with TEV protease.

Ensemble lipid mixing

A step-by-step protocol for SNARE protein purification and v-/t-SNARE vesicle reconstitution for lipid mixing experiments has been reported in our previous publication (26). The protein to lipid ratio was 1:200 for both t-SNARE and v-SNARE vesicles, by which approximately 100-200 copyies of SNARE proteins would be reconstituted to individual vesicles (27, 28). DiI-labeled t-SNARE vesicles and DiD-labeled v-SNARE vesicles were mixed at a molar ratio of 1:1. To demonstrate the activity of vesicle fusion via lipid mixing, we measured acceptor fluorescence intensity by FRET using a fluorescence spectrometer (Varian Cary). Wavelengths of 530 and 670 nm were used for excitation of donor (DiI) and emission of acceptor (DiD), respectively. All experiments were performed at 35 ^{o}C.

Single vesicle docking

A detailed protocol for this step has been previously described (29, 30). The PEGylated surface of the microfluidic chamber was incubated with neutravidin (Invitrogen) for 5 min and washed with buffer. The v-vesicles were immobilized on the surface with a 5-min incubation, and washed with buffer to remove free vesicles. Then, t-vesicles were injected and washed after 15 min of incubation. Docked

t-vesicles were excited by a 532-nm laser (Crystal laser) on a total internal reflection fluorescence microscopy (Nikon). The docking number per an imaging area (45 × 90 μm^2) was analyzed and averaged by using a customized program written in C++ (Microsoft).

RESULTS

To check the influence of double TMDs on fusion, we performed experiments to investigate how the hydrophobic mismatch changes the fusion rate. Firstly, the double TMDs of Syx 17 was hybridized with Syx 1 WT (named as Syx 1/17) to eliminate the residue sequences difference of their zipping domains. We then performed an ensemble lipid-mixing assay to study the influence of double TMDs on the fusion process (**Fig. 1A**) The fluorescence intensity produced by FRET between the donor and acceptor dyes in vesicles was measured for ~1800 s (**Fig. 1B**). The same v-SNARE vesicles reconstituted with Syb 2 were used for vesicles reconstituted with Syx 1 WT or Syx 1/17. During the whole course of fusion, the intensity of Syx 1 WT system is higher than that of Syx 1/17, indicating that the fusion rate of Syx 1 WT system is higher than that of Syx 1/17. By fitting the fluorescence intensity curve, we found that the fusion rate K of Syx 1 WT system is ~3.6-4.1 times as much as that of Syx 1/17. To eliminate the influence of double TMDs on vesicle docking, the rate-limiting step of ensemble experiments, we also performed the single-vesicle docking assay (**Fig. S2**). No difference on docking was observed (**Fig. S2B**), indicating that the reduced lipid mixing lies on the fusion step. Moreover, since the vesicle docking is induced by the interaction of SNARE domains, the result shown in **Fig. S2B** also implies the reconstituted level of t-SNARE proteins for Syx 1 WT and Syx 1/17 vesicles was similar and the fusion reduction was mainly caused by the difference of TMDs.

A theoretical model was introduced to investigate the influence of length mismatch between lipid thickness and TMDs on the membrane fusion. Three representative structures were used to capture the fusion process (**Fig. 2A)** (31). In the beginning state, the tilted TMDs of Syx and Syb formed bundles in the membrane respectively (**Fig. 2A**, α state); with the zipping of SNARE core helical structure, the TMDs rotated and moved along with membrane deformation (**Fig. 2A**, β state); after SNARE zipping finished, two opposed membranes merged and a fusion pore formed, the TMDs of Syx and Syb came to close contact (**Fig. 2A**, γ state). In our theoretical model, we described the fusion process with a reaction coordinate d, the distance between the tails of transmembrane domain, as shown in the state β of **Fig. 2A**. This distance stays at its minimum, $d_{\min}$, before fusion begins at the state α. The distance reaches its maximum, $d_{\max}=2b$, after fusion completes at the state of γ, where b is the length of TMDs. Because d monotonically increases from α to γ state, we could use a dimensionless parameter, $\xi(d)=(d-d_{\min})/(d_{\max}-d_{\min})$, to describe the fusion process. Note that $\xi(d)=0$ at state α and $\xi(d)=1$ at state γ.

The energy involved the fusion process was divided into three parts

$$E = E_t + E_{Zipping} + E_{pore} \quad (1)$$

in which E_t is the energy contribution of lipid-protein mismatch; $E_{Zipping}$ is the releasing energy by SNARE zipping; and E_{pore} is the energy cost of the membrane deformation to form a fusion pore. As described by previous studies, a mismatch may exist between the thickness of the membrane and the length of TMDs, which will tilt TMDs in the membrane after their insertion (17-19). For TMDs with lipid-protein mismatch, some hydrophobic region will extend out of membrane if the TMDs were to insert into the membrane vertically (**Fig. 2B**) and increase the interfacial energy of the extruded region. Thus, the TMDs prefer to insert into the membrane with a tilt angle θ_t to bury all the hydrophobic area

(**Fig. 2B**). Accordingly, the total interfacial energy varies with the tilt angle θ_t. Here, we assume that the tile angle θ_t changes linearly during TMD insertion into membrane during the fusion process, in which case, the tilt energy becomes

$$E_t = N_t E_{t0} \xi(d) \tag{2}$$

where N_t is the number of TMDs involving in the fusion process. For single SNARE, $N_t = 2$ (TMD from Syx1 WT and Syb). For two SNAREs, $N_t = 4$ etc.. E_{t0} is the tilt energy for one TMD change during the fusion process. The length of TMD and membrane composition can significantly influence the suitable tilt angle and energy profile (17, 19). According to previous studies (18, 19), the energy barrier, $E_{t0}^{'} = \sim 4.6 - 6.1 k_B T$ for tilt energy changes from the minimum to the maximum. As shown in **Fig. 2C**, when the fusion process finishes and Syx comes to close contact with Syb, both the TMDs insert in the membrane with a residual tilt angle θ_{t0} due to the radius of TMDs (**Fig. 2C**). The radius of membrane contour curvature R_m (**Fig. 2C**) was estimated in a range of 3-10 nm based on previous simulations and experiment results (13, 32-36), the radius of TMDs is $r = 0.35nm$ (13). Therefore, the residual tilt angle after the fusion process finishes can be calculated $\theta_{t0} = \arcsin(r/R_m)$ (**Fig. 2C**), and θ_{t0} comes to $\sim 2.0 - 6.7°$. As a result, the tilt energy changes during fusion process from α to γ state $E_{t0} = \sim 2.7 - 4.7 k_B T$ (18, 19).

The energy of each SNARE released during the fusion process is $E_0^{SNARE} = 35 k_B T$ (37). $E_{Zipping}$ is the energy of SNAREs zipping which are assumed to be linear with the normalized fusion process

$$E_{zipping} = N \cdot E_0^{SNARE} \cdot \frac{d - d_{\min}}{d_{\max} - d_{\min}} \tag{3}$$

Finally, E_{pore} is the energy cost to form a fusion pore on the membrane during the fusion process. This energy profile changes with the fusion process and could be fit by a Gauss function with an energy barrier of $E_0^{pore} = 34.3 k_B T$ (38). The maximum energy barrier was assumed to be located in the middle of the fusion process

$$E_{pore} = y_0 + E_0^{pore} e^{-\frac{\left[d-(d_{\min}+d_{\max})/2\right]^2}{2\omega^2}} \quad (4)$$

The parameters used in this study were listed in **Table 1**.

To calculate the fusion rate, according to the Kramers' theory (13, 39, 40), the reaction rate k can be written as

$$k = \frac{\sqrt{\phi_{well} \cdot \phi_{barrier}}}{f} e^{-\Delta E / k_B T} \quad (5)$$

where ΔE is the energy barrier of the reaction. ϕ_{well} and $\phi_{barrier}$ are the quadratic coefficients for the energy profile at the minimum and at the peak of the barrier, respectively. f is a constant related to the diffusion coefficient. k_B is the Boltzmann constant, and T is the absolute temperature. Finally, we got the fusion rate ratio between two reactions of i and j

$$\frac{k_i}{k_j} = \frac{\sqrt{\phi_{well}^i \cdot \phi_{barrier}^i}}{\sqrt{\phi_{well}^j \cdot \phi_{barrier}^j}} e^{-\left(\Delta E^i - \Delta E^j\right)/k_B T} \quad (6)$$

The total energy profiles during membrane fusion were calculated with different number of SNAREs. The energy profiles and energy barrier for N = 1-3 were shown in **Fig. 3A**. The energy barriers decrease with an increasing number of SNAREs taking part in the fusion process. When three or more SNAREs were involved in the fusion process, the energy barrier during the fusion process nearly vanished (see

189 **Fig. 3A**). As a result, fusion will finish rapidly, which is consistent with the previous study that efficient
190 fusion requires three or more SNARE complexes (41).
191
192 To investigate the influence of hydrophobic mismatch between the lipid bilayer and TMDs on the fusion
193 process, we calculate the energy profile with and without hydrophobic mismatch with two SNAREs
194 during fusion. Compared with fusion process without hydrophobic mismatch, the energy barrier of
195 fusion process with hydrophobic mismatch is $\sim 2.8 k_B T$ higher (**Fig. 3B**). At the beginning of fusion
196 with hydrophobic mismatch, the TMDs are tilted in the membrane (see α state in **Fig. 2A**). After the
197 formation of fusion pore, the TMDs of Syb and Syx contact with each other and will be almost
198 perpendicular to the membrane (see γ state in **Fig. 2A** and **Fig. 2C**). The energy profile changes and
199 the energy barrier increases if the lipid-protein mismatch was involved. Thus, the fusion process with
200 hydrophobic mismatch experiences a higher energy barrier and leads to a slower fusion rate.
201
202 To analyze our experimental results in **Fig. 1**, we investigated the influence of double TMDs with our
203 theoretical model. The tilt energy change during the fusion process with double TMDs is larger than that
204 of single TMD, which was mainly due to larger TMD numbers N_t. The calculated difference between
205 single TMD and double TMDs is shown in **Fig. S3**. The energy profile during the fusion process is
206 shown in **Fig. 4A**. When two SNAREs take part in the fusion process, the double TMDs increases the
207 fusion energy barrier and reduces fusion rate. The energy barrier of Syx 1/17 is $\sim 1.53 k_B T$ higher than
208 that of Syx 1 WT, so that the fusion rate of Syx1 WT is ~4.6 times higher than that of Syx 1/17,
209 consistent with the experimental result (**Fig. 1B**). Both our experimental and theoretical results showed
210 that double TMDs reduce fusion rate significantly, which could explain why the fusion process of
211 autophagosomes and lysosomes is slower than the fusion during neurotransmission (22, 42).

Considering the hydrophobic mismatch effect, we predict that, when 1-3 SNAREs were involved in the fusion process, the fusion rate of Syx 1 WT can be ~1.8-4.9 times higher than that of Syx 1/17 (**Fig. 4B**). The FRET experiment showed that the fusion rate of Syx 1 WT system is ~3.6-4.1 times higher than that of Syx 1/17. Since we used the physiological relevant level of lipids and proteins (43), our results indicate that the number of SNAREs involved in a general fusion process is likely to be 2 to 3 (see **Fig. 4B**).

DISCUSSION

The interplay between protein and membrane is essential for inducing and regulating membrane fusion (44). As the direct link between SNAREs and membrane, TMD stays the center of biophysical and biochemical researches of SNARE-mediated membrane fusion (45), especially for fusion pore opening (46). Previously, the TMD interaction of multiple Syx 1 proteins has been proposed for fusion pore opening (47). However, replacing the single TMD of Syx 1 with a lipid anchor showed no effect on synaptic transmission (22). To solve this issue, we studied how the hydrophobic mismatch between the membrane and TMD affects the fusion process by theoretical modeling and in vitro reconstitution experiments. The uniqueness of our study is adding an extra TMD to increase lipid-protein mismatch, instead of deleting TMD. Both of our theoretical and experimental results showed that the hydrophobic mismatch effect between the thickness of the membrane and the length of TMDs reduces the fusion rate.

Moreover, our theoretical modeling not only explains the role of double TMDs in reducing fusion rate but also reveals the number of SNAREs involved in fusion. The SNARE number involved in a fusion process is a hotspot in the fusion related researches (13, 41, 48-51), controversy still exists and the

235 proposed number range from one to some dozens (49). For example, some studies proposed that more
236 than a dozen of SNAREs were needed for fusion (48, 49). In contrast, it was also proposed that only a
237 small number of SNAREs can complete the fusion process (41, 50, 51). For example, Bogaart et al.
238 proposed that only one SNARE could lead to fusion (50), while some experimental results showed that
239 one to three SNAREs are sufficient for completing the membrane fusion (41, 51). Our results showed
240 that 2-3 SNAREs are involved in a general fusion process, which is consistent with previous studies (41,
241 49-51).

242

243 Author Contributions

244 D.L., B.J., and J.D. contributed to concept and design of this study. B.B. and D.L. performed theoretic
245 calculation. Z.T. performed and analyzed data for fusion and docking experiments. B.B., D.L., K.Z. B.J.,
246 and J.D. wrote manuscript.

247

248 Acknowledgments

249 The authors would like to thank M. Padolina for protein preparation. B.B., D.L., and B.J. were supported
250 by funds from the National Natural Science Foundation of China (NSFC 11932017, 11772054,
251 11772055, 11532009, and 11902051). D.L. was supported by the Fundamental Research Funds for the
252 Central Universities (Grant No. 2019QNA4060). K.Z. was supported by the School of Molecular Cell
253 Biology at the University of Illinois at Urbana-Champaign. J.D. was supported by the NIH
254 (R35GM128837).

References

1. Chernomordik, L. V., and M. M. Kozlov. 2008. Mechanics of membrane fusion. Nat Struct Mol Biol 15(7):675-683.
2. Cho, S., and H. von Gersdorff. 2013. Neuroscience: Faster than kiss-and-run. Nature 504(7479):220-221.
3. Fuhrmans, M., G. Marelli, Y. G. Smirnova, and M. Muller. 2015. Mechanics of membrane fusion/pore formation. Chem Phys Lipids 185:109-128.
4. Jahn, R., and R. H. Scheller. 2006. SNAREs--engines for membrane fusion. Nat Rev Mol Cell Biol 7(9):631-643.
5. Chen, Y. A., and R. H. Scheller. 2001. SNARE-mediated membrane fusion. Nat Rev Mol Cell Biol 2(2):98-106.
6. Wang, Y., L. Li, C. Hou, Y. Lai, J. Long, J. Liu, Q. Zhong, and J. Diao. 2016. SNARE-mediated membrane fusion in autophagy. Semin Cell Dev Biol 60:97-104.
7. Sutton, R. B., D. Fasshauer, R. Jahn, and A. T. Brunger. 1998. Crystal structure of a SNARE complex involved in synaptic exocytosis at 2.4 angstrom resolution. Nature 395(6700):347-353.
8. Stein, A., G. Weber, M. C. Wahl, and R. Jahn. 2009. Helical extension of the neuronal SNARE complex into the membrane. Nature 460(7254):525-528.
9. Itakura, E., C. Kishi-Itakura, and N. Mizushima. 2012. The hairpin-type tail-anchored SNARE syntaxin 17 targets to autophagosomes for fusion with endosomes/lysosomes. Cell 151(6):1256-1269.
10. Itakura, E., and N. Mizushima. 2013. Syntaxin 17: the autophagosomal SNARE. Autophagy 9(6):917-919.
11. Katsov, K., M. Muller, and M. Schick. 2004. Field theoretic study of bilayer membrane fusion. I. Hemifusion mechanism. Biophys J 87(5):3277-3290.
12. Jackson, M. B. 2009. Minimum membrane bending energies of fusion pores. J Membr Biol 231(2-3):101-115.
13. Jackson, M. B. 2010. SNARE complex zipping as a driving force in the dilation of proteinaceous fusion pores. J Membr Biol 235(2):89-100.
14. Ryham, R. J., T. S. Klotz, L. Yao, and F. S. Cohen. 2016. Calculating Transition Energy Barriers and Characterizing Activation States for Steps of Fusion. Biophys J 110(5):1110-1124.
15. Mostafavi, H., S. Thiyagarajan, B. S. Stratton, E. Karatekin, J. M. Warner, J. E. Rothman, and B. O'Shaughnessy. 2017. Entropic forces drive self-organization and membrane fusion by SNARE proteins. Proc Natl Acad Sci U S A 114(21):5455-5460.
16. Bu, B., Z. Tian, D. Li, and B. Ji. 2016. High Transmembrane Voltage Raised by Close Contact Initiates Fusion Pore. Front Mol Neurosci 9:136.
17. Strandberg, E., S. Esteban-Martin, A. S. Ulrich, and J. Salgado. 2012. Hydrophobic

mismatch of mobile transmembrane helices: Merging theory and experiments. Biochim Biophys Acta 1818(5):1242-1249.

18. Lee, J., and W. Im. 2008. Transmembrane helix tilting: insights from calculating the potential of mean force. Phys Rev Lett 100(1):018103.

19. Kim, T., and W. Im. 2010. Revisiting hydrophobic mismatch with free energy simulation studies of transmembrane helix tilt and rotation. Biophys J 99(1):175-183.

20. Milovanovic, D., A. Honigmann, S. Koike, F. Gottfert, G. Pahler, M. Junius, S. Mullar, U. Diederichsen, A. Janshoff, H. Grubmuller, H. J. Risselada, C. Eggeling, S. W. Hell, G. van den Bogaart, and R. Jahn. 2015. Hydrophobic mismatch sorts SNARE proteins into distinct membrane domains. Nat Commun 6:5984.

21. Killian, J. A. 1998. Hydrophobic mismatch between proteins and lipids in membranes. Bba-Rev Biomembranes 1376(3):401-416.

22. Zhou, P., T. Bacaj, X. Yang, Z. P. Pang, and T. C. Sudhof. 2013. Lipid-anchored SNAREs lacking transmembrane regions fully support membrane fusion during neurotransmitter release. Neuron 80(2):470-483.

23. Gong, J., Y. Lai, X. Li, M. Wang, J. Leitz, Y. Hu, Y. Zhang, U. B. Choi, D. Cipriano, R. A. Pfuetzner, T. C. Sudhof, X. Yang, A. T. Brunger, and J. Diao. 2016. C-terminal domain of mammalian complexin-1 localizes to highly curved membranes. Proc Natl Acad Sci U S A 113(47):E7590-E7599.

24. Lai, Y., U. B. Choi, Y. Zhang, M. Zhao, R. A. Pfuetzner, A. L. Wang, J. Diao, and A. T. Brunger. 2016. N-terminal domain of complexin independently activates calcium-triggered fusion. Proc Natl Acad Sci U S A 113(32):E4698-4707.

25. Lai, Y., J. Diao, D. J. Cipriano, Y. Zhang, R. A. Pfuetzner, M. S. Padolina, and A. T. Brunger. 2014. Complexin inhibits spontaneous release and synchronizes Ca2+-triggered synaptic vesicle fusion by distinct mechanisms. eLife 3:e03756.

26. Diao, J., L. Li, Y. Lai, and Q. Zhong. 2017. In Vitro Reconstitution of Autophagosome-Lysosome Fusion. Methods Enzymol 587:365-376.

27. Diao, J., Y. Ishitsuka, H. Lee, C. Joo, Z. L. Su, S. Syed, Y. K. Shin, T. Y. Yoon, and T. Ha. 2012. A single vesicle-vesicle fusion assay for in vitro studies of SNAREs and accessory proteins. Nature Protocols 7(5):921-934.

28. Kyoung, M. J., Y. X. Zhang, J. J. Diao, S. Chu, and A. T. Brunger. 2013. Studying calcium-triggered vesicle fusion in a single vesicle-vesicle content and lipid-mixing system. Nature Protocols 8(1):1-16.

29. Diao, J., D. J. Cipriano, M. Zhao, Y. Zhang, S. Shah, M. S. Padolina, R. A. Pfuetzner, and A. T. Brunger. 2013. Complexin-1 enhances the on-rate of vesicle docking via simultaneous SNARE and membrane interactions. J Am Chem Soc 135(41):15274-15277.

30. Diao, J., T. Y. Yoon, Z. Su, Y. K. Shin, and T. Ha. 2009. C2AB: a molecular glue for lipid vesicles with a negatively charged surface. Langmuir : the ACS journal of surfaces and colloids 25(13):7177-7180.

31. Han, J., K. Pluhackova, and R. A. Bockmann. 2017. The Multifaceted Role of SNARE Proteins in Membrane Fusion. Front Physiol 8:5.

32. Diao, J., P. Grob, D. J. Cipriano, M. Kyoung, Y. Zhang, S. Shah, A. Nguyen, M. Padolina, A. Srivastava, M. Vrljic, A. Shah, E. Nogales, S. Chu, and A. T. Brunger. 2012. Synaptic proteins promote calcium-triggered fast transition from point contact to full fusion. eLife 1:e00109.

33. Bu, B., M. Crowe, J. Diao, B. Ji, and D. Li. 2018. Cholesterol suppresses membrane leakage by decreasing water penetrability. Soft Matter 14(25):5277-5282.

34. Tsai, H. H., C. M. Chang, and J. B. Lee. 2014. Multi-step formation of a hemifusion diaphragm for vesicle fusion revealed by all-atom molecular dynamics simulations. Biochim Biophys Acta 1838(6):1529-1535.

35. Kawamoto, S., M. L. Klein, and W. Shinoda. 2015. Coarse-grained molecular dynamics study of membrane fusion: Curvature effects on free energy barriers along the stalk mechanism. J Chem Phys 143(24):243112.

36. Lai, Y., L. Zhao, B. Bu, X. Lou, D. Li, B. Ji, J. Liu, J. Diao, and Y. K. Shin. 2015. Lipid molecules influence early stages of yeast SNARE-mediated membrane fusion. Phys Biol 12(2):025003.

37. Li, F., F. Pincet, E. Perez, W. S. Eng, T. J. Melia, J. E. Rothman, and D. Tareste. 2007. Energetics and dynamics of SNAREpin folding across lipid bilayers. Nat Struct Mol Biol 14(10):890-896. Article.

38. Francois-Martin, C., J. E. Rothman, and F. Pincet. 2017. Low energy cost for optimal speed and control of membrane fusion. Proc Natl Acad Sci U S A 114(6):1238-1241.

39. Hänggi, P., P. Talkner, and M. Borkovec. 1990. Reaction-rate theory: fifty years after Kramers. Reviews of Modern Physics 62(2):251-341.

40. Kramers, H. A. 1940. Brownian motion in a field of force and the diffusion model of chemical reactions. Physica 7(4):284-304.

41. Shi, L., Q. T. Shen, A. Kiel, J. Wang, H. W. Wang, T. J. Melia, J. E. Rothman, and F. Pincet. 2012. SNARE proteins: one to fuse and three to keep the nascent fusion pore open. Science 335(6074):1355-1359. Research Support, Non-U.S. Gov't.

42. Watanabe, S., B. R. Rost, M. Camacho-Perez, M. W. Davis, B. Sohl-Kielczynski, C. Rosenmund, and E. M. Jorgensen. 2013. Ultrafast endocytosis at mouse hippocampal synapses. Nature 504(7479):242-247.

43. Takamori, S., M. Holt, K. Stenius, E. A. Lemke, M. Gronborg, D. Riedel, H. Urlaub, S. Schenck, B. Brugger, P. Ringler, S. A. Muller, B. Rammner, F. Grater, J. S. Hub, B. L. De Groot, G. Mieskes, Y. Moriyama, J. Klingauf, H. Grubmuller, J. Heuser, F. Wieland, and R. Jahn. 2006. Molecular anatomy of a trafficking organelle. Cell 127(4):831-846.

44. van den Bogaart, G., K. Meyenberg, H. J. Risselada, H. Amin, K. I. Willig, B. E. Hubrich, M. Dier, S. W. Hell, H. Grubmuller, U. Diederichsen, and R. Jahn. 2011. Membrane protein sequestering by ionic protein-lipid interactions. Nature 479(7374):552-555.

45. Tian, Z., J. Gong, M. Crowe, M. Lei, D. Li, B. Ji, and J. Diao. 2019. Biochemical studies of membrane fusion at the single-particle level. Prog Lipid Res 73(1):92-100.

46. Bao, H., D. Das, N. A. Courtney, Y. Jiang, J. S. Briguglio, X. Lou, D. Roston, Q. Cui, B. Chanda, and E. R. Chapman. 2018. Dynamics and number of trans-SNARE complexes determine nascent fusion pore properties. Nature 554(7691):260-263.

47. Han, X., C. T. Wang, J. Bai, E. R. Chapman, and M. B. Jackson. 2004. Transmembrane segments of syntaxin line the fusion pore of Ca2+-triggered exocytosis. Science 304(5668):289-292.

48. Karatekin, E., J. Di Giovanni, C. Iborra, J. Coleman, B. O'Shaughnessy, M. Seagar, and J. E. Rothman. 2010. A fast, single-vesicle fusion assay mimics physiological SNARE requirements. Proc Natl Acad Sci U S A 107(8):3517-3521.

49. Xu, W., B. Nathwani, C. Lin, J. Wang, E. Karatekin, F. Pincet, W. Shih, and J. E. Rothman. 2016. A Programmable DNA Origami Platform to Organize SNAREs for Membrane Fusion. J Am Chem Soc 138(13):4439-4447.

50. van den Bogaart, G., M. G. Holt, G. Bunt, D. Riedel, F. S. Wouters, and R. Jahn. 2010. One SNARE complex is sufficient for membrane fusion. Nat Struct Mol Biol 17(3):358-364.

51. Sinha, R., S. Ahmed, R. Jahn, and J. Klingauf. 2011. Two synaptobrevin molecules are sufficient for vesicle fusion in central nervous system synapses. Proc Natl Acad Sci U S A 108(34):14318-14323.

392 **Table 1**. The definitions and parameters for the theoretical model.

Symbol	Definition	Values	Ref
N	Number of SNARE complexes	1-3	(41)
r	Radius of TMDs	$3.5\,\text{Å}$	(13)
R_m	Radius of membrane contour curvature	3-10nm	(13, 32-35)
E_{t0}	Tilt energy change during fusion process	$\sim 2.7-4.7k_BT$	(18, 19)
E_b^{pore}	Energy to generate a membrane fusion pore	$34.3k_BT$	(38)
y_0	Gauss curvature parameter	$-1.01\,k_BT$	Fitting with (38)
E_0^{pore}	Gauss curvature parameter	$35.3\,k_BT$	Fitting with (38)
ω	Gauss curvature parameter	0.188nm	Fitting with (38)
E_{SNARE}	Energy provided by one SNARE protein	$35k_BT$	(37)

393

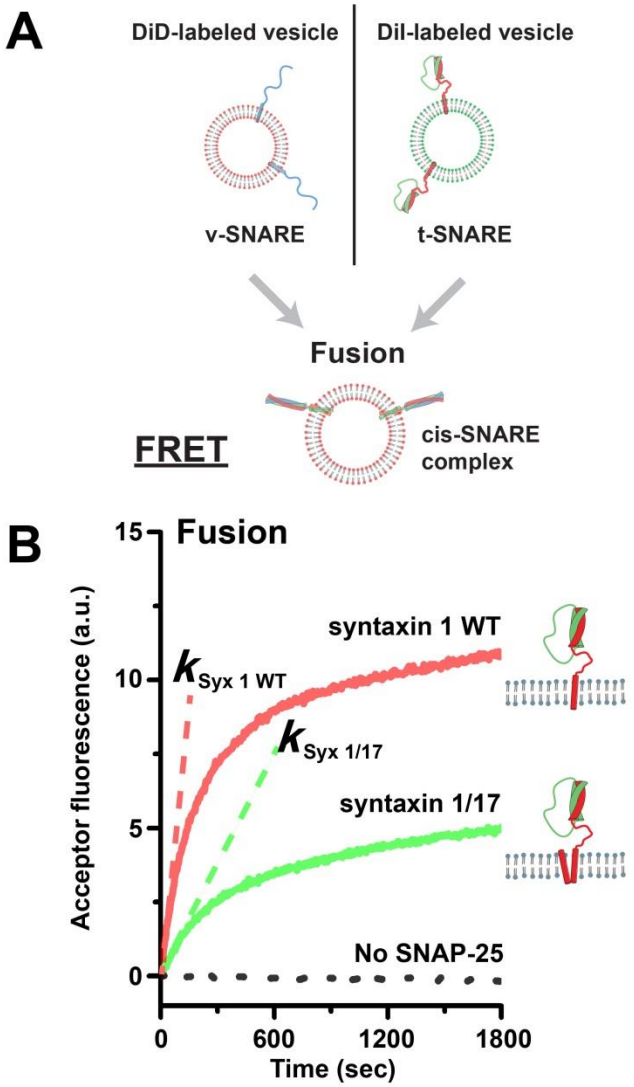

Figure 1. The double TMDs reduces fusion rate in vitro. (A) The illustration of v-vesicles and t-vesicles fusion. (B) Fusion of v-vesicles and t-vesicles reconstituted with syntaxin 1 wild-type (Syx 1 WT) or syntaxin 1 hybridized to a double TMDs of syntaxin 17 (Syx 1/17). The y axis is acceptor fluorescence intensity produced by FRET between the donor and acceptor dyes in vesicles, a measure of the activity of vesicle fusion with lipid mixing.

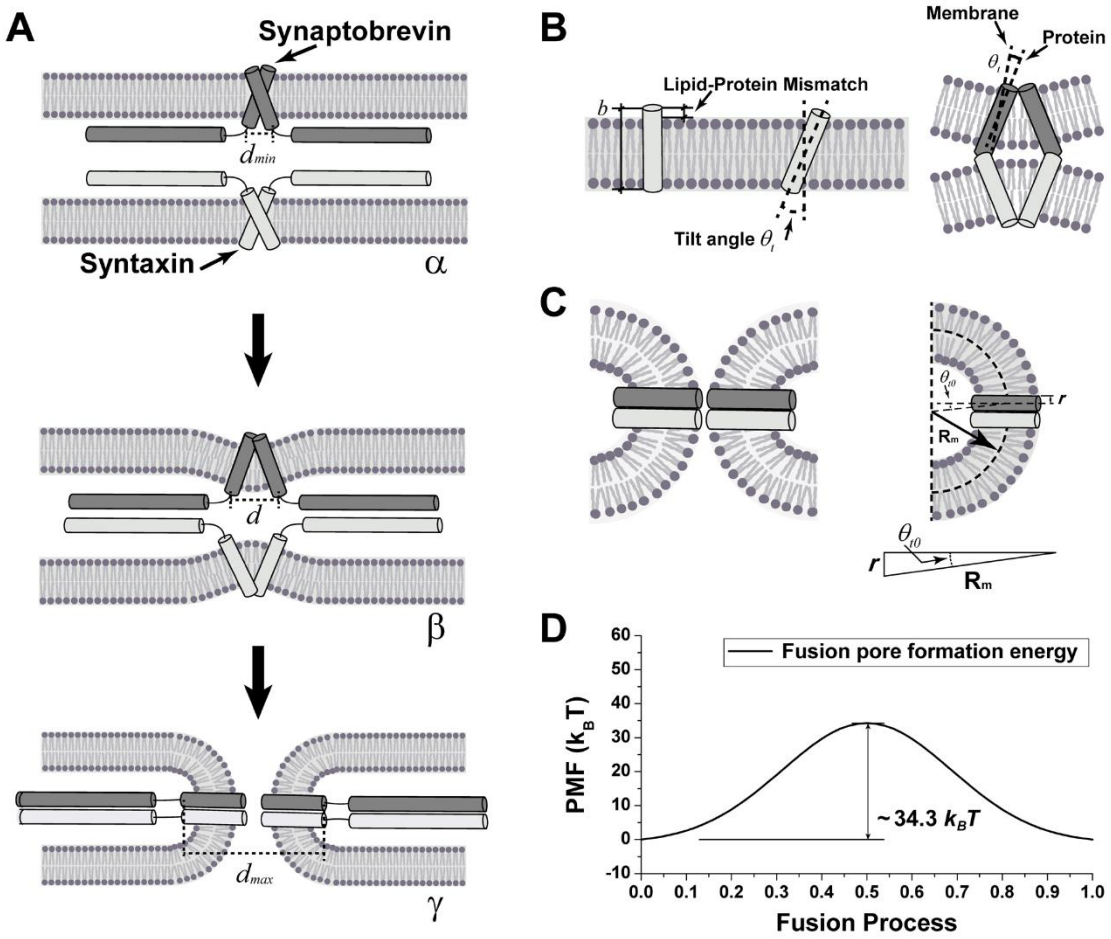

Figure 2. The fusion process with lipid-protein hydrophobic mismatch. (A) The representative structures of transition process from protein anchored in the membrane to fusion pore formation. TMDs rotated and moved, membrane deformed with fusion process from α to γ. d, $d_{\min}$, and $d_{\max}$ is the distance between the transmembrane domain's tails at different states, respectively. (B) The illustration of E_t energy contribution. E_t is the energy which represent the TMDs tilt (lipid-protein hydrophobic mismatch). b is the length of TMDs. θ_t is the tilt angle, which is the angle between the direction of TMDs and normal direction of membrane. (C) Illustration of lipid-protein mismatch interface in γ state. θ_{t0} is the residual tilt angle when the fusion process finished. R_m is the radius of membrane contour curvature. r is the radius of TMD. The residual tilt angle θ_{t0} can be calculated as $\theta_{t0} = \arcsin\left(r/R_m\right)$. (D) The profile of fusion pore formation energy E_{pore} as a function of the fusion process was set as a Gauss curvature (38).

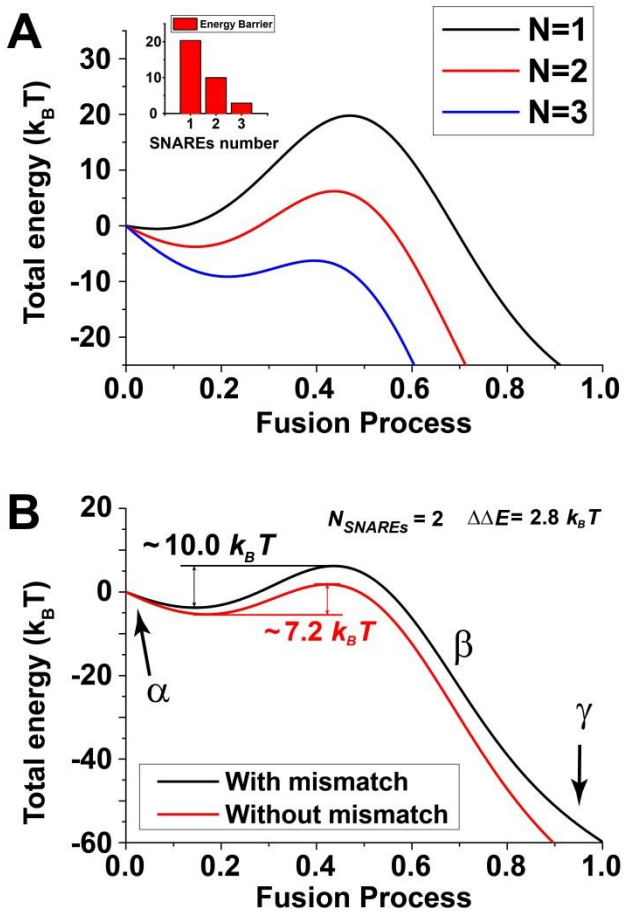

Figure 3. (A) The fusion energy profiles and barrier changed with different SNAREs number. (B) The energy profile of fusion process with and without mismatch as a function of fusion process. Two SNAREs were assumed to take part in the fusion process.

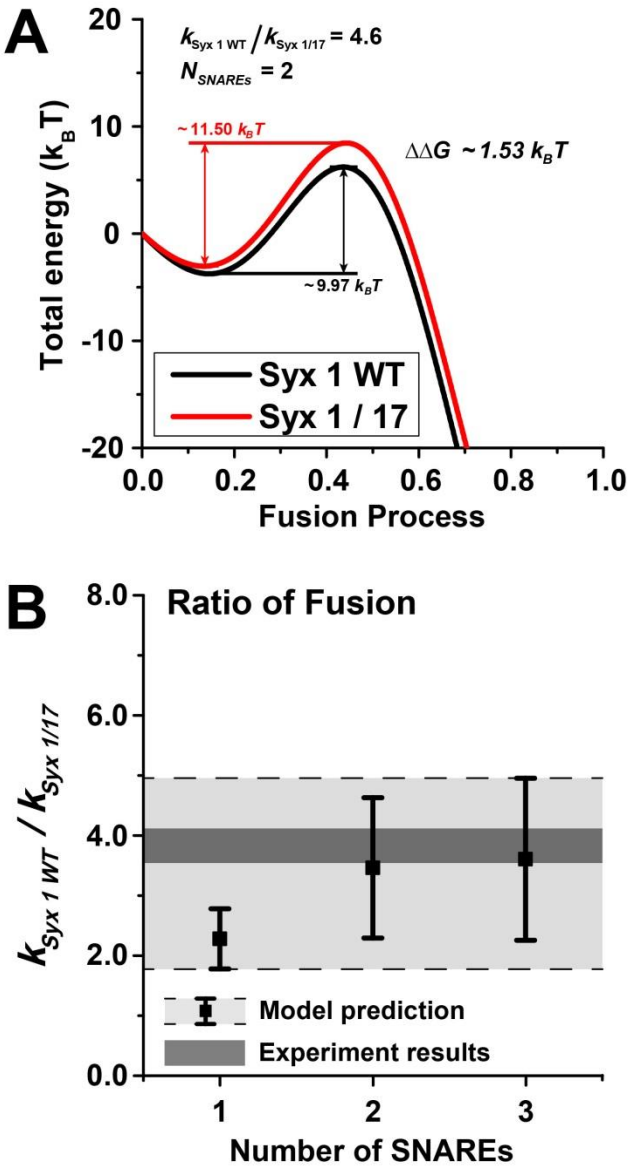

Figure 4. Theoretic analysis of fusion for Syx 1 WT and Syx 1/17. (A) The energy profiles of Syx 1 WT and Syx 1/17 as function of fusion process. Two SNAREs were assumed to take part in the fusion process. (B) The ratio of fusion velocity between Syx 1 WT and Syx 1/17 with various SNAREs number predicted by the theoretical model was compared with the experiment results. The light grey shadow region represented that tilt energy E_{t0} varies from 2.7 to 4.7 k_BT and SNAREs number varies from 1 to 3.